Article

Not peer-reviewed version

A Zinc Oxide Nanorod-Based Electrochemical Biosensor for the Detection of Tumor Markers in Saliva

Junrong Li , Yihao Ding , Yuxuan Shi , Zhiying Liu , Jun Lin , Rui Cao , Miaomiao Wang , Yushuo Tan , Xiaolin Zong , Zhan Qu * , Liping Du * , Chunsheng Wu *

Posted Date: 6 September 2024

doi: 10.20944/preprints202409.0447.v1

Keywords: carcinoembryonic antigen; oral squamous cell carcinoma; electrochemical; biosensor; saliva

Article

A Zinc Oxide Nanorod-Based Electrochemical Biosensor for the Detection of Tumor Markers in Saliva

Junrong Li [1,#], Yihao Ding [1,#], Yuxuan Shi [1,#], Zhiying Liu [1], Jun Lin [1], Rui Cao [1], Miaomiao Wang [1], Yushuo Tan [1], Xiaolin Zong [2], Zhan Qu [1,*], Liping Du [1,*] and Chunsheng Wu [1,*]

[1] Institute of Medical Engineering, Department of Biophysics, School of Basic Medical Sciences, Health Science Center, Xi'an Jiaotong University, Xi'an 710061, China;
[2] Jiashan JunYuan New Material Sci&Tech Co. Ltd., Jiashan 314100, China
* Correspondence: zhan.qu@xjtu.edu.cn (Z.Q.); duliping@xjtu.edu.cn (L.D.); wuchunsheng@xjtu.edu.cn (C.W.)
# These authors contributed equally.

Abstract: Biosensors have emerged as a promising tool for early detection of oral squamous cell carcinoma (OSCC) due to their rapid, sensitive, and specific detection of cancer biomarkers. Saliva is a non-invasive and easy-to-obtain biofluid that contains various biomarkers of OSCC, including carcinoembryonic antigen (CEA). In this study, an electrochemical biosensor for the detection of CEA in Saliva has been developed towards the diagnosis and early screening of OSCC. This biosensor utilized CEA-sensitive aptamer as sensitive elements. Fluorine-doped Tin Oxide (FTO) chip with surface modification of zinc oxide nanorod was employed as transducer. Electrochemical measurements were carried out to detect the responsive signals originated from the specific binding between aptamers and CEAs. The measurement results indicated that this biosensor was responsive to different concentrations of CEA ranging from 1 ng/mL to 80 ng/mL in a linear relationship. The limit of detection (LOD) was 0.75 ng/mL. This biosensor also showed very good specificity and regenerative capability. Stability testing over a 12-day period showed excellent performance of this biosensor. All the results demonstrated that this biosensor have great potential to be used for the detection of CEA in the saliva of OSCC patients. This biosensor provides a promising method for the rapid detection of CEA with convenience, which have great potential to be used as a new method for clinical diagnosis and early screening of OSCC.

Keywords: carcinoembryonic antigen; oral squamous cell carcinoma; electrochemical; biosensor; saliva

1. Introduction

Oral squamous cell carcinoma (OSCC) is one of the most common head and neck malignancies, accounting for more than 90% of all oral cancers[1,2]. Because the early symptoms of OSCC are not obvious or even asymptomatic, most OSCC is not detected and diagnosed until the late stage, and the mortality rate is high[3]. Survey data from the National Cancer Institute (NCI) show that the 5-year survival rate for patients with OCSCC is about 63% overall, with 83% in the early stage and 38% in the late stage[4,5]. Therefore, early and accurate diagnosis of OSCC is of great significance to improve the survival rate of patients and reduce the mortality rate.

At present, OSCC is mainly diagnosed by oral examination and tissue biopsy[6]. As the gold standard in diagnosis, tissue biopsy has irreplaceable value, but it is not suitable for the early diagnosis of OSCC due to its invasive nature, high cost, and possible infection close to normal tissues[6–9]. In recent years, liquid biopsy has shown important clinical value in the early diagnosis of tumors through the detection and analysis of biomarkers[10–12]. Carcinoembryonic antigen (CEA) is one of the most widely used tumor biomarkers. Studies have shown that the increase of CEA concentration in blood and saliva is related to the occurrence and development of OSCC, which can be used for early identification, efficacy judgment and prognosis monitoring of OSCC[13,14].

 doi:10.20944/preprints202409.0447.v1

Compared with blood testing, saliva testing has the advantages of non-invasive and painless sampling, simple and convenient, and low risk of contamination, and is more suitable for point-of-care testing (POCT)[15,16]. In addition, because saliva is more stable than blood, there are fewer interfering substances, and it is in direct contact with cancerous tissue, so the accuracy and specificity of the test is also higher[6,17]. Traditional CEA detection methods include enzyme-linked immunosorbent assay (ELISA), fluorescence spectrometry, colorimetry, chemiluminescence immunoassay, etc., which have many shortcomings such as low sensitivity and selectivity, time consuming, complex operation and high cost[18–20]. Therefore, it is particularly important and essential to develop a sensitive, accurate, simple, rapid and low-cost CEA detection method towards early diagnosis and screening of OSCC.

Electrochemical biosensors have great prospects for CEA detection due to their high sensitivity, convenience, and significant specificity[21,22]. For example, antibody-based electrochemical immunosensors have been widely studied in the determination of CEA. Although they are specific, they have disadvantages such as high cost and poor stability[23–25]. In contrast, aptamers are specially modified oligonucleotides, which have the advantages of small size, high affinity, strong stability, non-immunogenicity, easy preparation, low cost of synthesis and modification. Therefore, electrochemical biosensors based on aptamers have attracted much attention[26–28].

In recent years, nanomaterials have been widely used in the field of biosensors because of their superior physical and chemical properties[29–31]. Among them, zinc oxide (ZnO) nanomaterials have attracted much attention in the field of electrochemical biosensors due to their good biocompatibility, electron transfer properties, large specific surface area and non-toxicity, which effectively improve the sensitivity and responsiveness of biosensors[32,33]. In order to continuously optimize the performance of ZnO nanosensors, 3D ZnO nanostructures have attracted extensive attention in recent years[34–36]. The three-dimensional structure of ZnO nanocrystals has a higher specific surface area, which can effectively increase the contact area between the tested substance and the semiconductor material, improve the electron transfer rate and the fixing efficiency of the aptamer[33,37,38]. To effectively monitor CEA levels in saliva, aptamers need to be fixed to substrates such as carbon nanotubes and metal-organic frameworks[39,40]. In recent years, gold (Au), silver (Ag) and other metal nanoparticles (NPs) have been widely used to fix aptamers on the surface of sensor electrodes because of their good electrical conductivity and biocompatibility, large surface area, and easy synthesis[41,42]。Studies have shown that 3D biosensors based on 3D ZnO nanostructures and gold nanoparticles can effectively improve the sensitivity of detection[43].

In this study, an electrochemical biosensor based on aptamer-modified Fluorine-doped Tin Oxide (FTO)-ZnO-Au structure was developed to detect CEA in saliva for the early diagnosis and screening of OSCC. Firstly, the FTO-ZnO-Au structure was formed by modifying ZnO nanorods with gold nanoparticles, and the signal amplification system of aptamer-based biosensor was constructed. Then, the 3'-SH CEA-sensitive aptamer was covalently immobilized onto the surface of the electrode gold nanoparticle by Au-S bond to achieve the high-efficient coupling of sensitive elements with transducers. Electrochemical impedance spectroscopy (EIS) and cyclic voltammetry (CV) measurement were employed to characterize the biosensor preparation process as well as the performance testing of this biosensor for CEA detection. This electrochemical biosensor based on the FTO-ZnO-Au structure utilizes the three-dimensional structure constructed by ZnO-NRS to bind more aptamer molecules, and the highly specific binding of the aptamer to CEA also facilitates rapid and inexpensive CEA detection. The obtained results demonstrated the good performance of this electrochemical biosensor for CEA detection. This biosensor provides a new method for clinical diagnosis and early screening of OSCC by realizing rapid detection of CEA in a rapid and convenient manner. It is worth to note that FTO chips and CEA-sensitive aptamers used in this study are only for demonstration of the technical feasibility of the novel approach for CEA detection in saliva.

2. Materials and Methods

2.1. Materials and Reagents

 doi:10.20944/preprints202409.0447.v1

The following reagents were used as received: 6-mercapto-1-hexanol (MCH), tris-(2-carboxyethyl) phosphine hydrochloride (TCEP), bovine serum albumin (BSA) (purchased from Sigma-Aldrich, St.Louis, Missouri, USA). AREG Antigen (AREG-Ag), C-reactive protein (CRP), carcinoembryonic antigen (CEA) (purchased from Sangon Biotech, Shanghai, China). The wash buffer was phosphate buffer saline (PBS) (0.1 M, pH 7.4). Sulfuric acid (H_2SO_4), hydrochloric acid (HCl), sodium hydroxide (NaOH), hydrogen peroxide(H_2O_2), potassium ferricyanide ($K_3[Fe(CN)_6]$), potassium ferrocyanide ($K_4[Fe(CN)_6]$) and potassium chloride (KCl) (purchased from Sinopharm Chemical Reagent Co, Ltd, Shanghai, China). All reagents were analytical grade and used directly without further purification.

The CEA-sensitive aptamer sequence was chosen according to previous literatures[44], it had high affinity and specificity, and modified at the 3-terminus with a thiol group for the purpose of immobilization on the gold surface. The CEA-sensitive aptamer sequence was as follows:3′-SH-ATACC AGCTT ATTCA ATT-5′. The aptamers were dissolved in PBS buffer (pH 7.4) to certain concentrations for further experiments.

2.2. Preparation of FTO-ZnO-Au Structure

ZnO NRAs were prepared by hydrothermal method onto the FTO substrate. A thin film of ZnO was deposited onto the surface of FTO by radio frequency (RF) spurting as seeding layer. The hydrothermal deposition was carried out in the solution of equal volume of same concentration of 0.02 M $Zn(NO_3)_2$ and methenamine in a sealed beaker. The surface onto which the arrays was expected to grow was put downward, with temperature for the growth at 95℃ for 2 h. After growth, the substrate is removed from the container and rinsed with deionized water thoroughly, blown dry with N_2 for deposition a layer of Au by evaporation. Then, the prepared FTO-ZnO-Au structure can be used as electrochemical electrode for further experiments.

2.3. Immobilization of Aptamer

To covalently immobilize CEA-sensitive aptamer onto the gold surface of electrochemical electrode, TCEP offers a good linkage between the gilded groups and the aptamer. To achieve this, CEA-sensitive aptamer (10 μM, 18 μl), TCEP solution (10 mM, 3 μl), and NaAc solution (500 mM, 2 μl) were mixed, and the solution was stirred 1 h at room temperature allowing for the full reaction.

Prior to biosensor preparation, the bare gold electrodes (specs 1 × 1 cm, FTO-ZnO-Au) were pretreated for cleaning. Firstly, the electrodes were ultrasonically washed in 1 M NaOH solution for 30 min. Then, the electrodes were rinsed with ultrapure water and dried in a stream of nitrogen gas. Afterwards, the electrodes were ultrasonically washed in 1 M HCl solution for 5 min and rinsed with ultrapure water and dried in a stream of nitrogen gas. Next, the electrodes were ultrasonically washed in piranha solution (H_2O_2:H_2SO_4 = 1:3, 1 ml / 3 ml) for 8 min. Finally, the electrodes were rinsed with ultrapure water and dried in a stream of nitrogen gas.

The preparation process of the biosensor was schematically shown in Figure 1. First, 20 μl of previously prepared CEA-sensitive aptamer solution was added dropwise onto the surface of pretreated electrodes with FTO-ZnO-Au structure, which was incubated for 12 h at room temperature. Then, the electrode surface was rinsed with PBS buffer (PH 7.4) to remove the aptamers that was not bound to the gold surface, and dried naturally at room temperature. After that, previously prepared MCH solution (1 mM, 10 μl) was added dropwise onto the modified electrode surface, which was incubated for 30 min at room temperature to seal the non-specific binding sites. Then, the excess MCH on the electrode surface was removed with PBS buffer (PH 7.4) to obtain an electrochemical biosensor suitable for the detection of CEA. The prepared biosensors were stored in a refrigerator at 4℃ for future use.

Preprints.org (www.preprints.org) | NOT PEER-REVIEWED | Posted: 6 September 2024 doi:10.20944/preprints202409.0447.v1

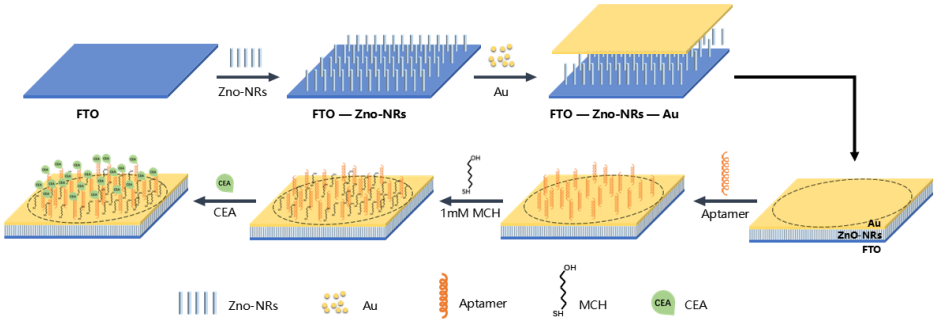

Figure 1. Schematic diagram showing the preparation process of electrochemical biosensors based on FTO-ZnO-Au structure and CEA-sensitive aptamer.

2.5. Electrical Measurement

The three-electrode system is a commonly used system in electrochemical experiments, especially in electroanalytical chemistry. In this study, the electrochemical measurement circuit adopted a three-electrode system, including a zinc oxide nanopillar gold electrode as the working electrode, a silver chloride electrode as the reference electrode, and a Pt wire as the counter electrode. The electrochemical measurements were performed on an electrochemical workstation (CHI600E, Chenhua, Shanghai, China), with a signal generator update rate of 10 MHz. The data acquisition used was two synchronous 16 bit high-resolution and low noise analog-to-digital converters, and the maximum speed for dual channel simultaneous sampling was 1 MHz. When the scanning speed of cyclic voltammetry was 1000 v/s, the potential increment was only 0.1 mV. When the scanning speed was 5000 v/s, the potential increment was 1 mV. The scanning voltage of parameter for CV was set to -0.4~0.8 v. The electrochemical impedance signal acquisition system used a 32-bit high-precision, high-resolution analog/digital signal converter with high dynamic range technology and a scanning voltage range of 14 V. The frequency range of parameter for EIS was set to 100 kHz ~100 MHz.

Electrical measurements were carried out in electrolyte containing 5 mM $K_3[Fe(CN)_6]$, 5 mM $K_4[Fe(CN)_6$ and 0.1 M KCl. Firstly, the electrochemical characterization of bare electrodes, adapter-modified electrodes, and sealed electrodes were measured separately. Next, the electrode surface was rinsed with PBS buffer (PH 7.4) and dried naturally at room temperature. Then, a certain concentration gradient CEA solution (5 ng/ml, 20 ng/ml, 50 ng/ml, 60 ng/ml, 80 ng/ml) was added dropwise onto the electrode surface, which was incubated for 1 h at room temperature. The electrochemical measurement of different concentration CEA were performed separately. After that, the electrochemical characterization of the electrodes, which were hydrolyzed with trypsin for 5 min at room temperature. Finally, the electrochemical characterization of the electrodes, which were incubated with 20 ng/ml CRP, BSA and Areg-Ag to test the specificity of this biosensor.

2.6. Signal Analysis

Accurate resistance values on the surface of the working electrode chip under different testing environments were analyzed using ZView software to fit and merge the measured electrochemical impedance spectra. Perform linear fitting and plot fitting curves for the resistance of electrodes incubated with different concentrations of CEA using SPSS 13.0. The electrochemical impedance map and cyclic voltammetry map were all plotted using Origin 8.0.

3. Results and Discussion

3.1. Characterization of Prepared FTO-ZnO-Au Structure

FTO-ZnO-Au structure was utilized as transducer for the development of electrochemical biosensor towards CEA detection. The surface with ZnO-NRs could improve the coupling efficiency

 doi:10.20944/preprints202409.0447.v1

between the transduce surface and aptamers. This could consequently improve the sensing performance for target detection. The surface gold layer was employed to facilitate the immobilization of thiol-modified aptamers onto the sensor surface via the strong Au-S bond. As a result, it is crucial to characterize the surface morphology of the FTO-ZnO-Au structure. In this study, atomic force microscope (AFM) and scanning electron microscope (SEM) were employed to characterize the electrode surface morphology. The characterization resulting images are shown in detail in Figure 2. As shown in Figure 2A, the SEM result indicated that ZnO-NRs are uniformly and densely distributed on the electrode surface. ZnO-NRs grow approximately vertically, with a hexagonal cross-section and a diameter of ~75nm. From AFM result shown in Figure 2B, it is indicated that ZnO-NRs grow uniformly, which further demonstrate the nano structure on sensor surface. Figure 2C shows SEM images of the surface of ZnO-NRs after deposition of a thin layer of chromium and gold. We can see that the chromium and gold layers are evenly distributed on the surface of ZnO-NRs by magnetron sputtering, and the morphology of ZnO-NRs can still be observed, which indicate that the three-dimensional structure of ZnO NRs is still retained on the electrode surface after gold deposition. All the results demonstrate that the FTO-ZnO-Au structure has been successfully prepared and is suitable for further experiments.

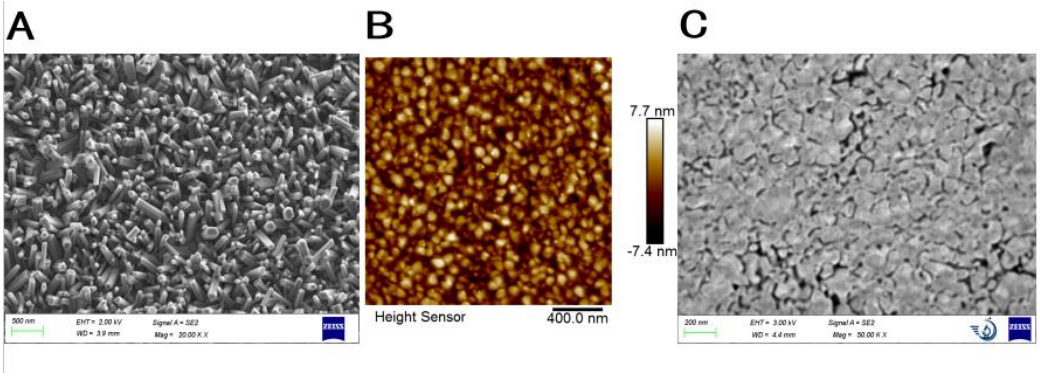

Figure 2. (A) SEM characterization of ZnO-NRs; (B) AFM characterization of FTO-ZnO-Au; (C) SEM image shows the surface of ZnO-NRs after the deposition of a thin layer of gold.

3.2. Electrochemical Characterization of Biosensor Preparation

The electrochemical biosensors were constructed by assembling CEA-sensitive aptamers on the electrode surface，and then treated with 1 mM MCH to block the non-specific sites on the surface of aptamer-modified electrode (Figure 1). Electrochemical impedance spectroscopy (EIS) and cyclic voltammetry (CV) were performed to describe its electrochemical characterization. For the Nyquist diagram, the semicircle diameter of the electrochemical impedance spectroscopy equals to the surface electron transfer resistance (R_{ct}). As shown in Figure 3A, the bare gold electrode showed a very small semicircle domain, which has almost no effect on electron transfer， exhibiting a very fast electron transfer process of $[Fe(CN)_6]^{3-/4-}$. When the aptamer was immobilized onto the electrode surface via Au-S bond, the R_{ct} value increased significantly. This is mainly due to the negatively charged aptamer acting as an electrostatic barrier in the $[Fe(CN)_6]^{3-/4-}$ system, hindering the electron transfer on the chip surface, which leads to an increase in the R_{ct} value. After MCH blocks the aptamer-modified electrode surface, the electron surface defects are repaired, which makes the electron surface layer more compact and further hinders the electron transfer, with a consequent further increase in R_{ct} value.

Cyclic voltammograms (CVs) were also carried out to describe the electrochemical characterization of surface modification process. As shown in Figure 3B, the peak current decreased with the connections of aptamers and the closure of MCH and increase in the peak to peak separation. This is mainly caused by the electrostatic repulsion between negative charges of the DNA aptamer and the anionic redox probe and the formation of the compact layer by the modification of MCH, which together results in the hamper of the interfacial electron transfer. The CV results were consistent to the EIS measurement results, further confirming the successful fabrication of the sensing interface.

 doi:10.20944/preprints202409.0447.v1

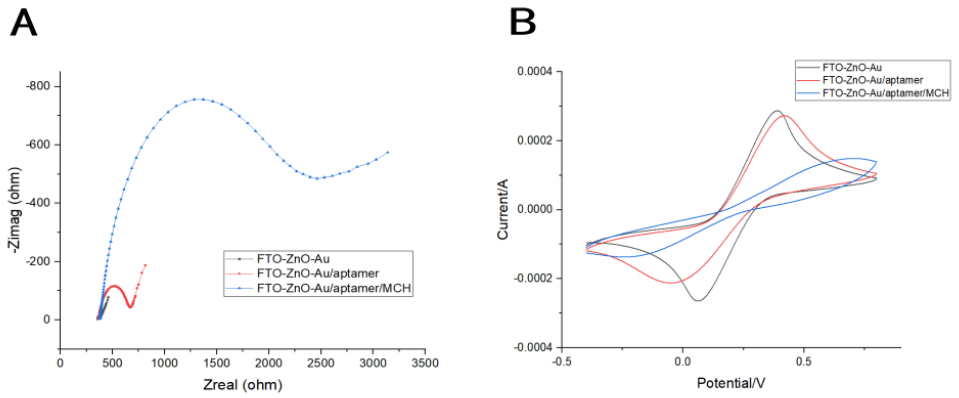

Figure 3. (A) The Nyquist plots and (B) CVs of the preparation steps of electrochemical biosensor based on CEA-sensitive aptamer.

3.3. Optimization of Measurement Conditions

To achieve the best detection performance, we optimized the relevant experimental parameters such as CEA-sensitive aptamer concentrations, incubation time of CEA-sensitive aptamer and reaction time. The more CEA aptamers attached onto the electrode surface, the greater R_{ct} value that could be detected.

Optimizing the time of incubate CEA-sensitive aptamer was an important step in building the electrochemical biosensors. As we can see from the curves shown in Figure 4A, when we use the CEA-sensitive aptamer with concentration of 5 μM for incubation, the peak current first increased and then decreased with the CEA-sensitive aptamer incubation time increased from 3 h to 20 h. Meanwhile, an excessive amount of incubation time might have a negative impact on the aptamer attachment onto the electrode surface. Therefore, in this study, 12 h was selected as the appropriate incubation time. Observing the trends depicted in Figure 4B, it was evident that the peak R_{ct} value also initially increased and later leveled off with the increase of CEA-sensitive aptamer concentrations from 1 μM to 40 μM. This indicated that the number of binding sites for CEA-sensitive aptamer on the electrode surface had reached saturation at the concentration of 10 μM. Therefore, a concentration of 10 μM for CEA-sensitive aptamer was deemed suitable for optimal performance.

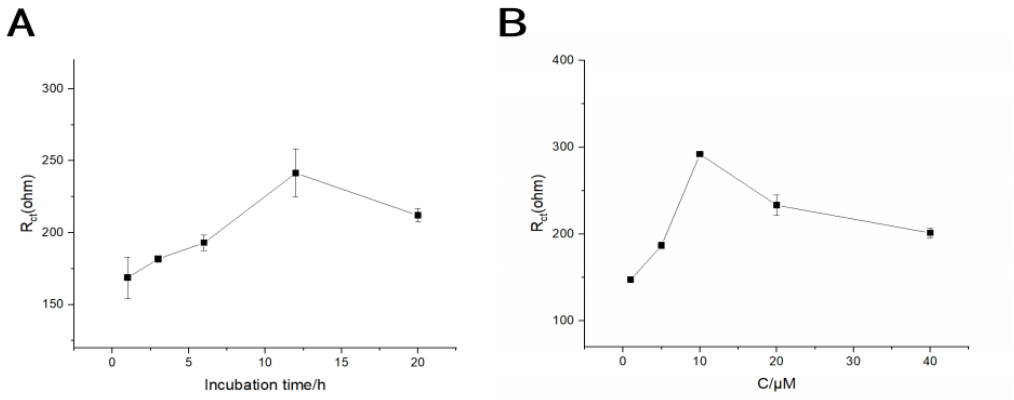

Figure 4. Optimization of biosensor preparation conditions. (A) Influence of incubation time of CEA-sensitive aptamer. (B) Influence of the concentrations of CEA-sensitive aptamer.

3.4. Analytical Performance Testing of Electrochemical Biosensor

When different concentrations of CEA were added under optimal conditions, as shown in Figure 5A, the electrode impedance increased with increasing CEA concentrations. The linear regression equation was R_{ct}(ohm) = 27.68 × C[CEA] +1335.69 (ng/mL) (R^2 = 0.9986). The linear range between the

 doi:10.20944/preprints202409.0447.v1

electrode impedance and CEA concentrations was from 1 to 80 ng/mL (Figure 5B), with a limit of detection (LOD) estimated to be 0.75 ng/mL (S/N = 3). Typically, the salivary CEA concentration in healthy individuals is found to be minimal (0~3 ng/mL), whereas in cancer patients, the CEA concentration is significantly elevated (>5 ng/ml), correlating with the presence of malignancies[45]. A prior investigation employing the enzyme-linked immunosorbent assay (ELISA) have reported salivary CEA levels of 42.6 ± 21.1 ng/mL in OSCC patients, contrasting with the levels of 22.6 ± 22.1 ng/mL observed in the control cohort[46]. Then, Table 1 concluded the detection performance of the developed electrochemical biosensor and the previously reported CEA biosensors. The developed electrochemical biosensor using the FTO-ZnO-Au nanostructure showed exceptional analytical performance, and characterized by a wide linear range, a lower LOD, and an exemplary linear correlation. In addition, compared with the anti-CEA antibody-based biosensors, the developed biosensor adopted an aptamer-based strategy to effectively improve the accuracy and reliability of detection.

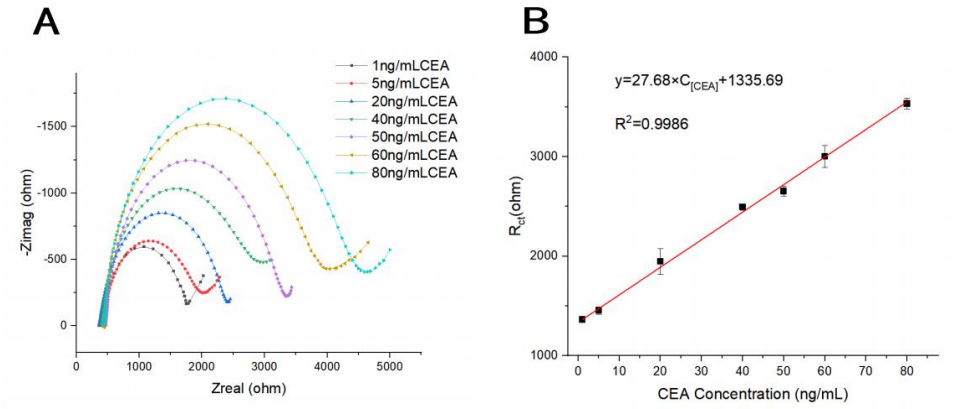

Figure 5. (A) EIS responses of the electrochemical biosensor for the detection of different concentrations of CEA. (B) Linear calibration plot between the electrode impedance and CEA concentrations.

3.5. Selectivity, Reproducibility, Stability and Regeneration of the Biosensor

To examine the selectivity of this electrochemical biosensor， we measured other proteins presented in human saliva, such as amphiregulin (Areg), C-reactive protein (CRP), Interleukin-8 (IL-8), and bovine serum albumin (BSA), which is commonly used for blocking. As shown in Figure 6A, only CEA showed significant responses, and other interferers only had subtle signal changes. These similar signal changes indicated that the interfering substances had little effect on the sensor, which proved that the developed biosensor have high specificity, which can be used for the specific detection of CEA. Secondly, we prepared 2 batches of 6 electrodes under the same conditions to detect 5 and 50 ng/mL CEA. The results were basically consistent, and the relative standard deviations (RSD) were 2.44 and 1.83%, respectively. The detection results showed that this biosensor had good reproducibility. At the same time, the stability of this biosensor was also investigated (Figure 6B). The results showed that after storage of 12 days at 4°C, compared with the current test signal on the initial experiment, the signal change rate was 94.52%. Therefore, this biosensor could be stored stably at least 12 days. This was attributed to the biocompatibility of ZnO-NRs stabilized the biological activity of the aptamers.

Table 1. Comparison of analytical methods for the detection of CEA.

Analytical method	Sensitive elements	Analytes	Linear ranges (ng/mL)	LOD (ng/mL)	R^2	Reference

 doi:10.20944/preprints202409.0447.v1

Fluoroimmunosensor	Anti-CEA antibody	CEA	1×10^{-1}~2.5 2.5~20	1.0×10^{-1}	0.988 0.996	[17]
Aptasensor	Aptamer	CEA	2×10^{-2}~6.0	3.25×10^{-1}	0.962	[47]
Electrochemical biosensor	Aptamer	CEA	5×10^{-2}~500	2.0×10^{-2}	0.989	[48]
Aptasensor	Aptamer	CEA	1~50	1.0	0.990	[49]
Fluoroimmunosensor	Anti-CEA antibody	CEA	7×10^{-1}~80	5.5×10^{-3}	0.993	[50]
Electrochemical biosensor	Aptamer	CEA	1~80	7.5×10^{-1}	0.999	This work

The regeneration of electrode surface is of great significance for reusable biosensors. In this study, we innovatively selected trypsin to digest CEA specifically bound to the aptamer, changing its structure and thus separating it from the aptamer to achieve the purpose of sensor regeneration, and achieved good results. The resistance of the sensor chip incubated with 5 and 60 ng/mL CEA for 5 min by trypsin digestion decreased to 67.04% of the original resistance, and the resistance increased to 89.81% of the original resistance after the same concentration of CEA was incubated again, indicating that the state of the chip surface after digestion basically returned to the state of unbound protein, and the activity of the aptamer was not affected.

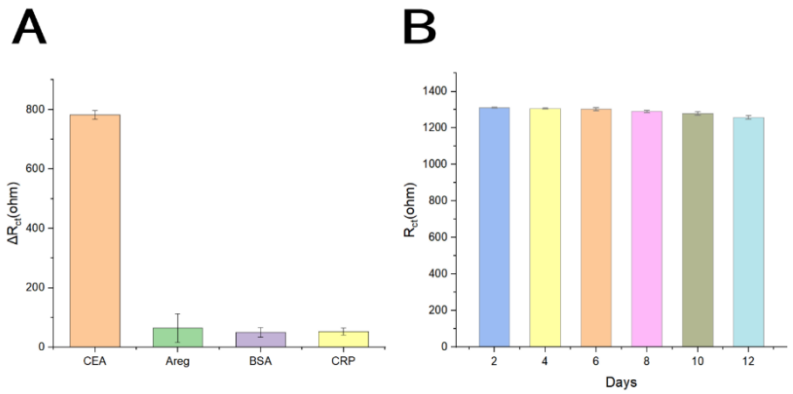

Figure 6. (A) Selectivity of the biosensor against CEA (20 ng/mL), Areg (50 ng/mL), BSA (50 ng/mL), CRP (20 ng/mL), and IL-8 (20 ng/mL). (B) Stability of the biosensor for 12 days of storage.

4. Conclusions

This study developed a simple and highly-sensitive biosensor for detecting the salivary biomarker CEA in OSCC. This biosensor is based on an FTO-ZnO-Au composite structure, where the corresponding ligands are immobilized on the electrode surface for target protein capture and signal detection. The combination of ZnO-NRs electrode and ligands offers multiple advantages, including high sensitivity, specificity, stability, and ease of fabrication. EIS and CV electrochemical characterization confirmed that the biosensor was successfully constructed and could effectively capture the target protein CEA. The results showed good linearity in the range of 5~80 ng/mL, with a LOD of 0.75 ng/ml. Experimentally determined tiny responses of AREG, CRP, IL-8 and BSA to the biosensor ensure that the aptamer sensor achieves specific detection of CEA in complex environments. Additionally, consistent detection results were obtained from multiple batches of sensors, confirming their reproducibility. Stability testing over a 15-day period showed excellent performance of the biosensor. Furthermore, the activity and detection performance of the ligands were minimally affected by pancreatic trypsin treatment, demonstrating the regenerative potential of the biosensor. This indicated that this biosensors has great potential for application in the detection

 doi:10.20944/preprints202409.0447.v1

of the tumour marker in saliva, and it is expected to develop a class of non-invasive, portable and highly-sensitive OSCC detection devices based on this biosensor.

Author Contributions: J.L.: Conceptualization, Investigation, Writing—Original draft preparation, Writing—Review and editing; Y.D.: Software, Investigation, Visualization; Y.S.: Software, Visualization; Z.L.: Visualization; J.L.: Software; R.C.: Investigation; M.W.: Visualization; Y.T.: Software; X.Z.: Investigation; Z.Q.: Writing—Review and editing, Software; L.D.: Conceptualization, Writing—Review and Editing, Supervision, Funding acquisition; C.W.: Writing—Review and Editing, Supervision, Funding acquisition, Project administration. All authors have read and agreed to the published version of the manuscript.

Funding: This research was funded by the National Natural Science Foundation of China (Grant Nos. 32071370, 32271427, and 32471433), and the S&T Program of Hebei (Gant No: 22321902D).

Conflicts of Interest: The authors declare no conflict of interest.

References

1. Badwelan, M.; Muaddi, H.; Ahmed, A.; Lee, K.T.; Tran, S.D. Oral Squamous Cell Carcinoma and Concomitant Primary Tumors, What Do We Know? A Review of the Literature. *Current Oncology* **2023**, *30*, 3721-3734, doi:10.3390/curroncol30040283
2. Bugshan, A.; Farooq, I. Oral squamous cell carcinoma: metastasis, potentially associated malignant disorders, etiology and recent advancements in diagnosis. *F1000Research* **2020**, *9*, doi:10.12688/f1000research.22941.1.
3. Li, Q.; Hu, Y.; Zhou, X.; Liu, S.; Han, Q.; Cheng, L. Role of Oral Bacteria in the Development of Oral Squamous Cell Carcinoma. *Cancers* **2020**, *12*, doi:10.3390/cancers12102797..
4. Al Feghali, K.A.; Ghanem, A.I.; Burmeister, C.; Chang, S.S.; Ghanem, T.; Keller, C.; Siddiqui, F. Impact of smoking on pathological features in oral cavity squamous cell carcinoma. *Journal of Cancer Research and Therapeutics* **2019**, *15*, 582-588, doi:10.4103/jcrt.JCRT_641_16.
5. Imbesi Bellantoni, M.; Picciolo, G.; Pirrotta, I.; Irrera, N.; Vaccaro, M.; Vaccaro, F.; Squadrito, F.; Pallio, G. Oral Cavity Squamous Cell Carcinoma: An Update of the Pharmacological Treatment. *Biomedicines* **2023**, *11*, doi:10.3390/biomedicines11041112.
6. Chakraborty, D.; Natarajan, C.; Mukherjee, A. Advances in oral cancer detection. *Adv Clin Chem* **2019**, *91*, 181-200, doi:10.1016/bs.acc.2019.03.006.
7. Khurshid, Z.; Zafar, M.S.; Khan, R.S.; Najeeb, S.; Slowey, P.D.; Rehman, I.U. Role of Salivary Biomarkers in Oral Cancer Detection. *Advances in clinical chemistry* **2018**, *86*, 23-70, doi:10.1016/bs.acc.2018.05.002.
8. Abati, S.; Bramati, C.; Bondi, S.; Lissoni, A.; Trimarchi, M. Oral Cancer and Precancer: A Narrative Review on the Relevance of Early Diagnosis. *Int J Environ Res Public Health* **2020**, *17*, doi:10.3390/ijerph17249160.
9. Goldoni, R.; Scolaro, A.; Boccalari, E.; Dolci, C.; Scarano, A.; Inchingolo, F.; Ravazzani, P.; Muti, P.; Tartaglia, G. Malignancies and Biosensors: A Focus on Oral Cancer Detection through Salivary Biomarkers. *Biosensors* **2021**, *11*, doi:10.3390/bios11100396.
10. Jayanthi, V.; Das, A.B.; Saxena, U. Recent advances in biosensor development for the detection of cancer biomarkers. *Biosens Bioelectron* **2017**, *91*, 15-23, doi:10.1016/j.bios.2016.12.014.
11. Cho, S.; Yang, H.C.; Rhee, W.J. Simultaneous multiplexed detection of exosomal microRNAs and surface proteins for prostate cancer diagnosis. *Biosens Bioelectron* **2019**, *146*, 111749, doi:10.1016/j.bios.2019.111749.
12. Wu, L.L.; Zhang, Z.L.; Tang, M.; Zhu, D.L.; Dong, X.J.; Hu, J.; Qi, C.B.; Tang, H.W.; Pang, D.W. Spectrally Combined Encoding for Profiling Heterogeneous Circulating Tumor Cells Using a Multifunctional Nanosphere-Mediated Microfluidic Platform. *Angew Chem Int Ed Engl* **2020**, *59*, 11240-11244, doi:10.1002/anie.201914468.
13. Zheng, J.; Sun, L.; Yuan, W.; Xu, J.; Yu, X.; Wang, F.; Sun, L.; Zeng, Y. Clinical value of Naa10p and CEA levels in saliva and serum for diagnosis of oral squamous cell carcinoma. *J Oral Pathol Med* **2018**, *47*, 830-835.
14. Rajguru, J.P.; Mouneshkumar, C.D.; Radhakrishnan, I.C.; Negi, B.S.; Maya, D.; Hajibabaei, S.; Rana, V. Tumor markers in oral cancer: A review. *J Family Med Prim Care* **2020**, *9*, 492-496, doi:10.4103/jfmpc.jfmpc_1036_19.
15. Zarrin, P.S.; Jamal, F.I.; Roeckendorf, N.; Wenger, C. Development of a Portable Dielectric Biosensor for Rapid Detection of Viscosity Variations and Its In Vitro Evaluations Using Saliva Samples of COPD Patients and Healthy Control. *Healthcare (Basel)* **2019**, *7*, doi:10.3390/healthcare7010011.
16. Senf, B.; Yeo, W.-H.; Kim, J.-H. Recent Advances in Portable Biosensors for Biomarker Detection in Body Fluids. *Biosensors* **2020**, *10*, doi:10.3390/bios10090127.
17. Li, Y.; Hu, S.; Chen, C.; Alifu, N.; Zhang, X.; Du, J.; Li, C.; Xu, L.; Wang, L.; Dong, B. Opal photonic crystal-enhanced upconversion turn-off fluorescent immunoassay for salivary CEA with oral cancer. *Talanta* **2023**, *258*, doi:10.1016/j.talanta.2023.124435.

18. Qin, W.; Wang, K.; Xiao, K.; Hou, Y.; Lu, W.; Xu, H.; Wo, Y.; Feng, S.; Cui, D. Carcinoembryonic antigen detection with "Handing"-controlled fluorescence spectroscopy using a color matrix for point-of-care applications. *Biosensors and Bioelectronics* **2017**, *90*, 508-515, doi:10.1016/j.bios.2016.10.052.
19. Rouhi, J.; Kakooei, S.; Sadeghzadeh, S.M.; Rouhi, O.; Karimzadeh, R. Highly efficient photocatalytic performance of dye-sensitized K-doped ZnO nanotapers synthesized by a facile one-step electrochemical method for quantitative hydrogen generation. *Journal of Solid State Electrochemistry* **2020**, *24*, 1599-1606, doi:10.1007/s10008-020-04695-y.
20. Wang, K.; Yang, J.; Xu, H.; Cao, B.; Qin, Q.; Liao, X.; Wo, Y.; Jin, Q.; Cui, D. Smartphone-imaged multilayered paper-based analytical device for colorimetric analysis of carcinoembryonic antigen. *Analytical and Bioanalytical Chemistry* **2020**, *412*, 2517-2528, doi:10.1007/s00216-020-02475-1.
21. Wang, L.; Xiong, Q.; Xiao, F.; Duan, H. 2D nanomaterials based electrochemical biosensors for cancer diagnosis. *Biosensors and Bioelectronics* **2017**, *89*, 136-151, doi:10.1016/j.bios.2016.06.011.
22. Zhang, C.; Zhang, S.; Jia, Y.; Li, Y.; Wang, P.; Liu, Q.; Xu, Z.; Li, X.; Dong, Y. Sandwich-type electrochemical immunosensor for sensitive detection of CEA based on the enhanced effects of Ag NPs@CS spaced Hemin/rGO. *Biosens Bioelectron* **2019**, *126*, 785-791, doi:10.1016/j.bios.2018.11.039.
23. Paniagua, G.; Villalonga, A.; Eguílaz, M.; Vegas, B.; Parrado, C.; Rivas, G.; Díez, P.; Villalonga, R. Amperometric aptasensor for carcinoembryonic antigen based on the use of bifunctionalized Janus nanoparticles as biorecognition-signaling element. *Analytica Chimica Acta* **2019**, *1061*, 84-91, doi:10.1016/j.aca.2019.02.015.
24. Shamsuddin, S.H.; Gibson, T.D.; Tomlinson, D.C.; McPherson, M.J.; Jayne, D.G.; Millner, P.A. Reagentless Affimer- and antibody-based impedimetric biosensors for CEA-detection using a novel non-conducting polymer. *Biosensors and Bioelectronics* **2021**, *178*, doi:10.1016/j.bios.2021.113013.
25. Song, Y.; Chen, K.; Li, S.; He, L.; Wang, M.; Zhou, N.; Du, M. Impedimetric aptasensor based on zirconium-cobalt metal-organic framework for detection of carcinoembryonic antigen. *Mikrochim Acta* **2022**, *189*, 338, doi:10.1007/s00604-022-05427-x.
26. Hashkavayi, A.B.; Raoof, J.B.; Ojani, R. Preparation of Epirubicin Aptasensor Using Curcumin as Hybridization Indicator: Competitive Binding Assay between Complementary Strand of Aptamer and Epirubicin. *Electroanalysis* **2017**, *30*, 378-385, doi:10.1002/elan.201700645.
27. Byun, J. Recent Progress and Opportunities for Nucleic Acid Aptamers. *Life* **2021**, *11*, doi:10.3390/life11030193.
28. Zhao, H.; Ming, T.; Tang, S.; Ren, S.; Yang, H.; Liu, M.; Tao, Q.; Xu, H. Wnt signaling in colorectal cancer: pathogenic role and therapeutic target. *Molecular Cancer* **2022**, *21*, doi:10.1186/s12943-022-01616-7.
29. Li, J.; Yang, F.; Chen, X.; Fang, H.; Zha, C.; Huang, J.; Sun, X.; Mohamed Ahmed, M.B.; Guo, Y.; Liu, Y. Dual-ratiometric aptasensor for simultaneous detection of malathion and profenofos based on hairpin tetrahedral DNA nanostructures. *Biosensors and Bioelectronics* **2023**, *227*, doi:10.1016/j.bios.2022.114853.
30. Maral, M.; Erdem, A. Carbon Nanofiber-Ionic Liquid Nanocomposite Modified Aptasensors Developed for Electrochemical Investigation of Interaction of Aptamer/Aptamer–Antisense Pair with Activated Protein C. *Biosensors* **2023**, *13*, doi:10.3390/bios13040458.
31. Zhang, X.-W.; Du, L.; Liu, M.-X.; Wang, J.-H.; Chen, S.; Yu, Y.-L. All-in-one nanoflare biosensor combined with catalyzed hairpin assembly amplification for in situ and sensitive exosomal miRNA detection and cancer classification. *Talanta* **2024**, *266*, doi:10.1016/j.talanta.2023.125145.
32. Lv, S.; Zhang, K.; Zhu, L.; Tang, D. ZIF-8-Assisted NaYF4:Yb,Tm@ZnO Converter with Exonuclease III-Powered DNA Walker for Near-Infrared Light Responsive Biosensor. *Anal Chem* **2020**, *92*, 1470-1476, doi:10.1021/acs.analchem.9b04710.
33. Que, M.; Lin, C.; Sun, J.; Chen, L.; Sun, X.; Sun, Y. Progress in ZnO Nanosensors. *Sensors* **2021**, *21*, doi:10.3390/s21165502.
34. Shetti, N.P.; Bukkitgar, S.D.; Reddy, K.R.; Reddy, C.V.; Aminabhavi, T.M. ZnO-based nanostructured electrodes for electrochemical sensors and biosensors in biomedical applications. *Biosens Bioelectron* **2019**, *141*, 111417, doi:10.1016/j.bios.2019.111417.
35. Xia, Y.; Chen, Y.; Tang, Y.; Cheng, G.; Yu, X.; He, H.; Cao, G.; Lu, H.; Liu, Z.; Zheng, S.Y. Smartphone-Based Point-of-Care Microfluidic Platform Fabricated with a ZnO Nanorod Template for Colorimetric Virus Detection. *ACS Sens* **2019**, *4*, 3298-3307, doi:10.1021/acssensors.9b01927.
36. Sinha, K.; Chakraborty, B.; Chaudhury, S.S.; Chaudhuri, C.R.; Chattopadhyay, S.K.; Das Mukhopadhyay, C. Selective, Ultra-Sensitive, and Rapid Detection of Serotonin by Optimized ZnO Nanorod FET Biosensor. *IEEE Transactions on NanoBioscience* **2022**, *21*, 65-74, doi:10.1109/tnb.2021.3112534.
37. Wang, Z.L. From nanogenerators to piezotronics—A decade-long study of ZnO nanostructures. *MRS Bulletin* **2012**, *37*, 814-827, doi:10.1557/mrs.2012.186.
38. Khan, M.; Nagal, V.; Masrat, S.; Tuba, T.; Alam, S.; Bhat, K.S.; Wahid, I.; Ahmad, R. Vertically Oriented Zinc Oxide Nanorod-Based Electrolyte-Gated Field-Effect Transistor for High-Performance Glucose Sensing. *Analytical Chemistry* **2022**, *94*, 8867-8873, doi:10.1021/acs.analchem.1c05630.

39. Lv, M.; Zhou, W.; Tavakoli, H.; Bautista, C.; Xia, J.; Wang, Z.; Li, X. Aptamer-functionalized metal-organic frameworks (MOFs) for biosensing. *Biosens Bioelectron* **2021**, *176*, 112947, doi:10.1016/j.bios.2020.112947.
40. Wang, Z.; Dai, L.; Yao, J.; Guo, T.; Hrynsphan, D.; Tatsiana, S.; Chen, J. Enhanced adsorption and reduction performance of nitrate by Fe–Pd–Fe3O4 embedded multi-walled carbon nanotubes. *Chemosphere* **2021**, *281*, doi:10.1016/j.chemosphere.2021.130718.
41. Chen, Y.; Wang, A.-J.; Yuan, P.-X.; Luo, X.; Xue, Y.; Feng, J.-J. Three dimensional sea-urchin-like PdAuCu nanocrystals/ferrocene-grafted-polylysine as an efficient probe to amplify the electrochemical signals for ultrasensitive immunoassay of carcinoembryonic antigen. *Biosensors and Bioelectronics* **2019**, *132*, 294-301, doi:10.1016/j.bios.2019.02.057.
42. Jouyandeh, M.; Sajadi, S.M.; Seidi, F.; Habibzadeh, S.; Munir, M.T.; Abida, O.; Ahmadi, S.; Kowalkowska-Zedler, D.; Rabiee, N.; Rabiee, M.; et al. Metal nanoparticles-assisted early diagnosis of diseases. *OpenNano* **2022**, *8*, 100104, doi:https://doi.org/10.1016/j.onano.2022.100104.
43. Kim, H.-M.; Park, J.-H.; Lee, S.-K. Fiber optic sensor based on ZnO nanowires decorated by Au nanoparticles for improved plasmonic biosensor. *Scientific Reports* **2019**, *9*, doi:10.1038/s41598-019-52056-1.
44. Luo, C.; Wen, W.; Lin, F.G.; Zhang, X.H.; Gu, H.S.; Wang, S.F. Simplified aptamer-based colorimetric method using unmodified gold nanoparticles for the detection of carcinoma embryonic antigen. *Rsc Advances* **2015**, *5*, 10994-10999, doi:10.1039/c4ra14833a.
45. Joshi, S.; Kallappa, S.; Kumar, P.; Shukla, S.; Ghosh, R. Simple diagnosis of cancer by detecting CEA and CYFRA 21-1 in saliva using electronic sensors. *Scientific Reports* **2022**, *12*, doi:10.1038/s41598-022-19593-8.
46. Honarmand, M.H.; Farhad-Mollashahi, L.; Nakhaee, A.; Nehi, M. Salivary Levels of ErbB2 and CEA in Oral Squamous Cell Carcinoma Patients. *Asian Pac J Cancer Prev* **2016**, *17*, 77-80.
47. Xu, Z.; Wang, C.; Ma, R.; Sha, Z.; Liang, F.; Sun, S. Aptamer-based biosensing through the mapping of encoding upconversion nanoparticles for sensitive CEA detection. *The Analyst* **2022**, *147*, 3350-3359, doi:10.1039/d2an00669c.
48. Wang, Y.; Luo, J.; Liu, J.; Sun, S.; Xiong, Y.; Ma, Y.; Yan, S.; Yang, Y.; Yin, H.; Cai, X. Label-free microfluidic paper-based electrochemical aptasensor for ultrasensitive and simultaneous multiplexed detection of cancer biomarkers. *Biosensors and Bioelectronics* **2019**, *136*, 84-90, doi:10.1016/j.bios.2019.04.032.
49. Shahbazi, N.; Hosseinkhani, S.; Ranjbar, B. A facile and rapid aptasensor based on split peroxidase DNAzyme for visual detection of carcinoembryonic antigen in saliva. *Sensors and Actuators B: Chemical* **2017**, *253*, 794-803, doi:10.1016/j.snb.2017.06.024.
50. Yu, Q.; Wang, X.; Duan, Y. Capillary-Based Three-Dimensional Immunosensor Assembly for High-Performance Detection of Carcinoembryonic Antigen Using Laser-Induced Fluorescence Spectrometry. *Analytical Chemistry* **2014**, *86*, 1518-1524, doi:10.1021/ac402973n.